

Electromagnetically induced transparency in a superconducting three-level system

Mika A. Sillanpää^{1,*}, Jian Li¹, Katarina Cicak², Fabio Altomare², Jae I. Park², Raymond W. Simmonds², G. S. Paraoanu¹, and Pertti J. Hakonen¹

¹*Helsinki University of Technology, Low Temperature Laboratory, Puumiehenukja 2B, Espoo, FIN-02015 HUT Finland*

²*National Institute of Standards and Technology, 325 Broadway, Boulder CO 80305, USA*

When a three-level quantum system is irradiated by an intense coupling field resonant with two of the three possible transitions, the resonant absorption of the system from its ground state by an additional radiation field is suppressed. This effect, where the population is trapped in the ground state, is known in quantum optics as "electromagnetically induced transparency". When the coupling field is detuned from resonance, the resonant absorption peak splits to form an "Autler-Townes doublet". We observe these phenomena in a superconducting Josephson phase qubit, which can be considered an "artificial atom" with a multilevel quantum structure. These observations are qualitatively described by a simple model restricted to three energy levels. A full solution of the master equation including higher levels provides excellent agreement with all the experimental data.

PACS numbers: 67.57.Fg, 47.32.-y

Superconducting qubits [1] have recently been employed as a testing ground for quantum mechanics in a nearly macroscopic system. The interaction of the effective two-level system with a resonant cavity has attracted a lot of attention [2, 3, 4, 5]. However, Josephson junction-based quantum systems can also possess higher quantum states or energy levels, beyond the two-level approximation, and these have received much less attention. For driven Rabi oscillations between the lowest two levels of a phase qubit, these higher states can reduce the apparent Rabi frequency at large drive powers [6, 7] as the energy leaks out of the subspace spanned by the ground state $|0\rangle$ and the first excited state $|1\rangle$. Recently, the second excited state $|2\rangle$ has been used in order to help characterize the fidelity of single quantum bit (qubit) gate operations [8].

In atomic physics and quantum optics, various experiments have utilized the naturally occurring multilevel state structure of "real" atoms. A system accessing just three energy levels can display a rich variety of phenomena. Coherent population trapping, electromagnetically induced transparency (EIT) [10], Autler-Townes splitting [11], and stimulated Raman adiabatic passage [12], have been thoroughly investigated with atoms, and recently, also with solid-state quantum dots [13, 14]. It is intriguing to demonstrate some of these phenomena using macroscopic quantum states in a superconducting-based framework. Phase qubits in particular are well-suited for this purpose because they have a simple ladder-type energy level structure as well as a measurement process that is fast and state specific.

In a phase qubit (see Fig. 1(a)), a single Josephson junction, capacitively shunted with C_J , having an effective linear inductance $L_J = (\Phi_0/2\pi)^2/E_J$, where E_J is the Josephson energy, and Φ_0 is the flux quantum, has been inserted into a superconducting loop. The loop inductance $L > L_J$ is chosen so that local minima

are formed in a one-dimensional energy potential $E_{\text{pot}} = (\Phi - \Phi_{\text{ext}})^2/2L - E_J \cos(2\pi\Phi/\Phi_0)$ controllable by an externally applied flux Φ_{ext} . For this experiment, there are approximately ten energy levels residing within one of these local minima as shown in Fig. 1(b).

Consider the three lowest energy levels in Fig. 1(b). We denote the transition frequencies between energy levels i and j as $\omega_{ji} = 2\pi f_{ji}$. Two microwave fields are present; a weak probe tone ω_p that is nearly resonant with ω_{10} and detuned an amount $\Delta_p = \omega_{10} - \omega_p$, and a strong coupling tone ω_c that is nearly resonant with ω_{21} (detuned by $\Delta_c = \omega_{21} - \omega_c$). The amplitude of these tones leads to corresponding Rabi "flopping" frequencies denoted by Ω_{21} and Ω_{10} . In atomic physics, the occupation of higher energy levels will often decay into a continuum of states, but here, the occupation of the higher levels will decay merely to the lower levels of this ladder or cascade-type configuration as seen in Fig. 1(b). This can be contrasted with the so-called "lambda" configuration familiar in atomic systems, where the state $|2\rangle$ would be lower in energy than the state $|1\rangle$. We denote the inter-level relaxation rates in our system by Γ_{21} and Γ_{10} . The rate Γ_{20} is a forbidden dipole transition due to the anharmonicity of the energy potential.

In the qubit's eigenbasis $|n\rangle$, the Hamiltonian takes the form $H = \sum_{n=0}^2 E_n |n\rangle\langle n| + \Omega_p \cos(\omega_p t) |1\rangle\langle 0| + \Omega_c \cos(\omega_c t) |2\rangle\langle 1| + \text{h.c.}$ In the rotating frame, neglecting counter-rotating terms, the Hamiltonian takes the form

$$H = \begin{bmatrix} 0 & \Omega_p/2 & 0 \\ \Omega_p/2 & \Delta_p & \Omega_c/2 \\ 0 & \Omega_c/2 & \Delta_p + \Delta_c \end{bmatrix}. \quad (1)$$

This Hamiltonian is familiar in atomic physics and has been used to describe coherent population trapping [15] and EIT [10]. Analogous phenomena have been predicted for superconducting qubits [16, 17], however, experimental measurements have not been forthcoming until now

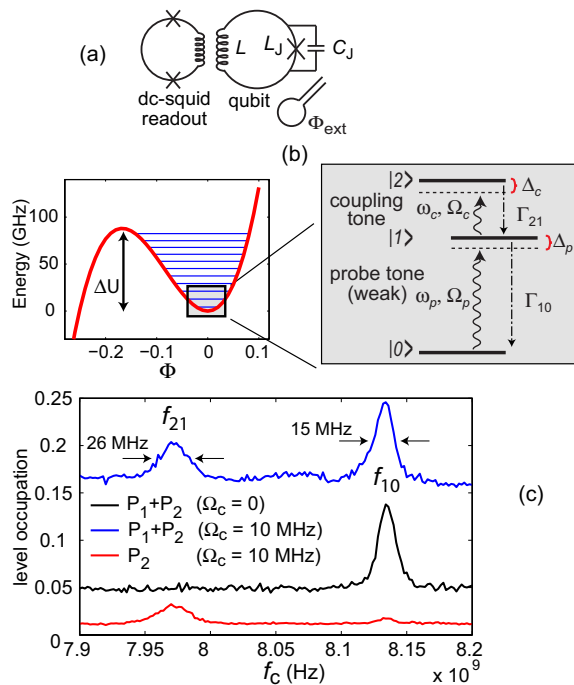


FIG. 1: (a) Schematics of the phase qubit and a nearby dc-squid for single-shot readout [9, 19] and on-chip flux coil; (b) Energy levels in the local potential minimum at $\Phi \sim \Phi_0$ given for the flux bias point $\Phi_{\text{ext}} \sim -0.42 \Phi_0$ used in the experiment. The zoom illustrates the cascade configuration of the three lowest levels used to generate electromagnetically induced transparency and the Autler-Townes splitting. The (strong) coupling field ω_c connects energy levels $|2\rangle$ and $|1\rangle$, and the weaker probe field f_p , whose resonant absorption becomes blocked due to the coupling field, connects $|1\rangle$ and $|0\rangle$. The corresponding Rabi drive amplitudes are denoted by Ω_c and Ω_p , respectively. Generally, both tones are detuned from the respective transitions by Δ_c and Δ_p ; (c) Two-tone microwave spectroscopy to reveal the two lowest transitions $f_{10} = 8.135$ GHz and $f_{21} = 7.975$ GHz (see text for details).

[18].

When both the coupling and probe tones are resonant with their corresponding transitions ($\Delta_c = \Delta_p = 0$), one of the eigenstates of Eq. (1) is the "dark state" $\Psi_0 = \cos(\Theta)|0\rangle - \sin(\Theta)|2\rangle$, where $\tan(\Theta) = \Omega_p/\Omega_c$. Note that this expression does not include the intermediate state $|1\rangle$. Thus, under these conditions, the system can no longer absorb radiation at the probe tone and becomes "transparent". Next, we describe experiments demonstrating this phenomenon for the multilevel superconducting phase qubit shown in Fig. 1.

The qubit sample was made by the use of optical lithography and standard Al-AlO_x-Al ion-mill tunnel junctions on a sapphire substrate. As compared to Ref. [3], the junction size was reduced by a factor of two in order to reduce the number of microscopic TLS defects within the tunnel barrier [19]. The experiments were per-

formed at 25 mK in a dilution cryostat. The qubit state is measured with a nanosecond-wide flux pulse as described in Ref. [3]. The measure pulse reduces the potential barrier ΔU (Fig. 1(b)) so that the resultant energy level at the top of this barrier, if occupied, has a high probability of tunneling out of the local minimum. Calibration of the measure pulse amplitude for the first excited state gives its population P_1 , and also leads to a residual tunneling probability P_0 out of the ground state of approximately 5%. Using this calibration, we also measure the population $P_1 + P_2$, when the second excited state $|2\rangle$ is occupied. To measure P_2 independently, we calibrate the measure pulse amplitude so that the residual tunneling probability P_1 out of $|1\rangle$ is approximately 5%.

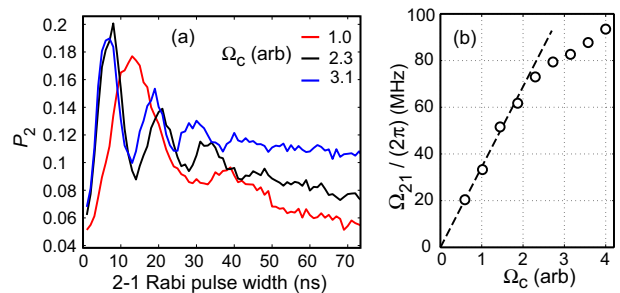


FIG. 2: Driven Rabi oscillations between energy levels $|2\rangle$ and $|1\rangle$. (a) Excited state probability P_2 as a function of the width of a pulse resonant with f_{21} (this pulse follows a π pulse resonant with f_{10} , see text); (b) the frequency of the Rabi oscillations Ω_{21} as a function of the coupling drive amplitude Ω_c . The dashed line is a fit to the linear portion of the data.

We operate the phase qubit at a center frequency $f_{10} = 8.135$ GHz where there are no visible TLS defects over a 1 GHz bandwidth. At high microwave powers, we spectroscopically observe a two-photon absorption peak, $f_{20}/2 = 8.06$ GHz. In order to identify the transition frequency f_{21} , we simultaneously apply two weak microwave tones. We set the probe tone f_p to resonantly pump the f_{10} transition while we vary the coupling tone f_c . We obtain a peak in the spectrum when $f_c = f_{21} = 7.975$ GHz for different measure pulse calibrations as shown in Fig. 1(c). The full spectroscopic data (not shown) for f_{10} and f_{21} as a function of the dc flux bias can be fit well to theory in order to extract the qubit parameters L_J and C_J , including any flux offsets. We also perform time-domain measurements (Fig. 2) by first applying a π pulse at f_{10} in order to populate $|1\rangle$ followed immediately by a pulse resonant with f_{21} of varying length. We obtain coherent Rabi oscillations of the second excited state P_2 , where the population flops between $|2\rangle$ and $|1\rangle$. In Fig. 2(b), we show the Rabi frequency Ω_{21} of these oscillations for several different coupling drive amplitudes Ω_c . A linear relationship between the Rabi frequency and drive amplitude survives up to about $\Omega_{21} \sim 70$ MHz, indicating that a three-level model is sufficient to describe

the dynamics up to this drive [6, 7].

We made independent measurements of the inter-level decay rates Γ_{21} and Γ_{10} (Fig. 1(b)) by preparing population in either $|2\rangle$ or $|1\rangle$, using sufficiently slow (~ 10 ns wide) π pulses in order to avoid population leakage to the higher levels, and observing energy decay in time domain. This gave $\Gamma_{21} = 11$ MHz and $\Gamma_{10} = 7$ MHz. The widths δf_{ij} of the spectroscopy peaks in Fig. 1 (c) give the pure dephasing rates $\Gamma_{10}^\varphi = 3.5$ MHz, $\Gamma_{21}^\varphi = 6$ MHz, according to $\delta f_{ij} = \Gamma_{ij} + 2\Gamma_{ij}^\varphi$.

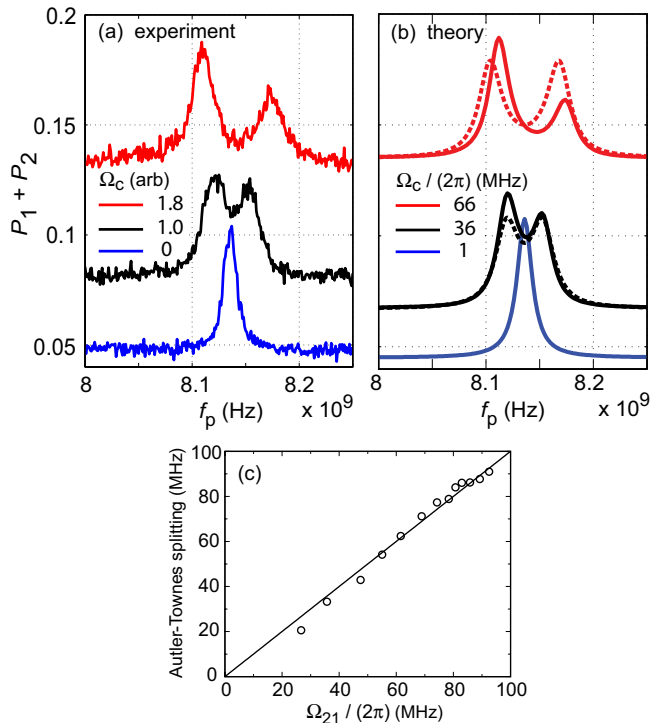


FIG. 3: Demonstration of electromagnetically induced transparency (EIT) in a multilevel phase qubit system. Plotted is the excited-level population $P_1 + P_2$ at different amplitudes of the coupling field, which cancels the resonant absorption of a weak probe field $\Omega_p = 3$ MHz. (a) experiment; (b) theory. Solid lines are the full simulation (see text), dashed lines (shifted vertically) represent the analytical line-shape from Eq. (2); (c) splitting as a function of the independently measured Rabi frequency Ω_{21} (from Fig. 2(b)). The solid line demonstrates the expected identity between the two quantities.

As discussed earlier, the "dark state" is expected to occur when both the coupling and probe tones are resonant with their corresponding transitions ($\Delta_c = \Delta_p = 0$). We expect this condition to be visible as a reduced population of the first excited state P_1 . In our cascade level configuration, energy decay from $|2\rangle$ reduces the effectiveness of the transparency by populating $|1\rangle$. Therefore, we increase the coupling tone amplitude so that $\Omega_c \gg \Omega_p$, and the dark state approximates the ground state. We find that the probe tone absorption peak begins to split,

forming a dip at $f_p = f_{10}$. The fact that the linewidth of this dip is broader than the linewidth of the f_{10} absorption peak, is another indication of the middle level $|1\rangle$ receiving population.

The characteristic features of EIT can be investigated further by determining the stationary states of the driven multilevel system by use of the Markovian master equation for the qubit's reduced density matrix ρ : $i\hbar\dot{\rho} = [H, \rho] + \mathcal{L}[\rho]$. The relaxation term $\mathcal{L}[\rho]$ includes the measured inter-level relaxation rates Γ_{21} and Γ_{10} as well as pure dephasing. If we restrict ourselves to the first three energy levels, neglect fast oscillating terms, assume $\Delta_c = 0$, a relatively large coupling amplitude ($\Omega_c \gg (\Omega_p, \Gamma_{21}, \Gamma_{10})$), and solve the resulting algebraic equations, we obtain a measured excited state population:

$$P_1 + P_2 = \rho_{11} + \rho_{22} = \frac{\Omega_p^2}{\Gamma_{10}} \times \frac{4\Delta_p^2(\lambda_{10} + \Gamma_{10}^\varphi) + \Omega_c^2(\Gamma_{10} + 2\lambda_{21})}{16\Delta_p^4 + [\Omega_c^2 + 4\lambda_{21}\lambda_{10}]^2 - 8\Delta_p^2[\Omega_c^2 - 2(\lambda_{21}^2 + \lambda_{10}^2)]} \quad (2)$$

where $\lambda_{ij} = \Gamma_{ij} + \Gamma_{ij}^\varphi$. The splitting of the absorption peak has a characteristic line shape which is not just a sum of two Lorentzians. The stationary off-diagonal elements of the density matrix when $\Delta_c = \Delta_p = 0$ indicate the coherence of the trapped population: $\rho_{01} = 2i\Gamma_{10}\rho_{11}/\Omega_p$. In Fig. 3(b), we find good agreement between the experimental data and the predictions from Eq. (2). In order to get the best fit, we have adjusted the value of Ω_c by about +10% from that of the independently measured Rabi frequency Ω_{21} .

The size of the splitting can be understood in terms of the Autler-Townes doublet [11, 21, 22] known in atomic physics. If we treat the amplitude of the probe tone as a small perturbation in Eq. (1), we obtain eigenenergies of the driven system: $\epsilon_{\pm} = \omega_{10} + \Delta_c/2 \pm \sqrt{\Delta_c^2 + \Omega_c^2}/2$. These energy levels are excited from the ground state using the probe tone. When $\Delta_c = 0$, the doublet is spaced by the coupling Rabi amplitude Ω_c . In Fig. 3(c), this splitting is plotted as a function of the independently measured Ω_{21} (from Fig. 2(b)), confirming their identity. By scanning the frequencies of the probe and coupling tones, one expects to find that the Autler-Townes doublet will exhibit an avoided crossing centered at $(\omega_{10}, \omega_{21})$. We display the results from this type of a measurement in Fig. 4 with the Autler-Townes eigenvalues plotted as white solid lines. Here, the experiment is performed with the same coupling amplitude as for the middle (black) curve shown in Fig. 2(a). Again we find good agreement for the simple three-level model when operating in the linear regime of the driven Rabi oscillations at $\Omega_{21} = 36$ MHz (Fig. 2(b)).

The vanishing intensity of the lower right leg of the Autler-Townes avoided crossing in Fig. 4 can be explained by considering the matrix element $\sin(\phi/2)$ con-

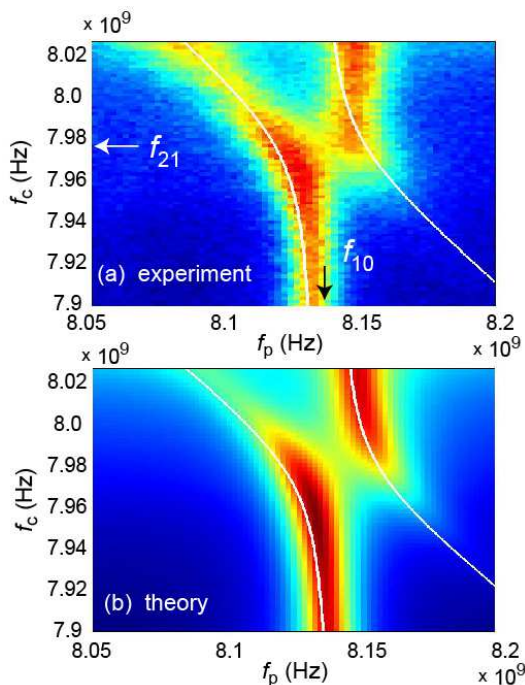


FIG. 4: Autler-Townes splitting in the three-level phase qubit, for a corresponding coupling field amplitude of $\Omega_c \rightarrow \Omega_{21} = 36$ MHz, and probe amplitude $\Omega_p = 5$ MHz. Resonances in the driven system exhibit an avoided crossing as a function of the detuning of the coupling field (vertical axis) and the probe field (horizontal axis). The white lines mark the expected transitions from the three-level Autler-Townes model. (a) measured excited-level population $P_1 + P_2$; (b) five-level simulation.

necting the driven eigenstates with the ground state, where the mixing angle is given by $\tan(\phi) = \Omega_c/2\Delta_c$. As the detuning Δ_c increases, this matrix element decreases so that the intensity of the split peak on the right also decreases, in agreement with the experimental data. However, the opposite, upper left leg shows a decreasing then increasing intensity with detuning. This can be attributed to an additional two-photon process, which becomes favorable when the probe tone reaches the two-photon resonance at 8.06 GHz, also causing an enhancement of the base level.

For the Hamiltonian of Eq. (1), we have assumed that both microwave fields couple only to their intended transitions, namely the coupling tone ω_c drives ω_{21} and the probe ω_p drives ω_{10} . In reality, the microwave fields cross-couple to both transitions. The strong coupling tone drives the f_{10} transition with a cross-coupling strength Ω_c^x , which contributes to the occupation of the first excited state, $P_1 = \frac{1}{2}\Omega_c^x \left[(\Delta_c + \omega_{10} - \omega_{21})^2 + \Omega_c^x \right]$, raising the base-level in Fig. 3(b) when far from f_{10} . For our weakly anharmonic potential, we estimate that the cross-coupling is $\Omega_c^x \simeq \Omega_c/\sqrt{2}$. When $\Omega_{21} = 36$ MHz, (middle (black) curve in Fig. 3, Fig. 4), the cross-coupling is

negligible. However, for strong coupling amplitudes corresponding to $\Omega_c = 66$ MHz (top (red) curves in Fig. 3) approaching the limitations of the three-level model, we must include the cross-coupling in order to correctly account for the position and symmetry of the Autler-Townes doublet.

Thus far, our simple three-level model has qualitatively accounted for the EIT behavior and the resulting Autler-Townes splitting in good agreement with the experimental data. Next, we provide a more accurate description of the system based on a full simulation that can quantitatively account for the multilevel nature of the phase qubit system. We solve the Markovian master equation including the first five energy levels of the system and also including the cross-coupling of the drive tones. The results are shown along side the experimental data in Fig. 3(b) and Fig. 4(b). We find excellent agreement without any fitting parameters. The simulation correctly captures the asymmetry of the splitting (Fig. 3(a)), which is a combination of the effects of the higher levels and cross-coupling, as well as the intensity vanishing of the left and right branches as a function of detuning as seen in Fig. 4(b).

In summary, we have observed phenomena characteristic of three-level systems familiar in atomic physics, namely electromagnetically induced transparency and Autler-Townes splitting, but in a superconducting Josephson junction-based quantum system. The results contribute to a general scientific effort that seeks to demonstrate quantum mechanical behavior in progressively more macroscopic and diverse systems. They also pave the way towards quantum information processing using higher-dimensional Hilbert spaces [23].

This work was financially supported by the Academy of Finland. NIST collaborators are supported by NIST and IARPA.

* Electronic address: Mika.Sillanpaa@iki.fi

- [1] Y. Nakamura, Yu. A. Pashkin, and J. S. Tsai, *Nature* **398**, 786 (1999).
- [2] A. Wallraff, *et al.*, *Nature* **431**, 162 (2004).
- [3] M. A. Sillanpää, J. I. Park, and R. W. Simmonds, *Nature* **449**, 438 (2007).
- [4] M. Hofheinz, *et al.*, *Nature* **454**, 310 (2008).
- [5] L. S. Bishop, J. M. Chow, J. Koch, A. A. Houck, M. H. Devoret, E. Thuneberg, S. M. Girvin, and R. J. Schoelkopf, *Nature Phys.* **5**, 105 (2009).
- [6] J. Claudon, F. Balestro, F. W. Hekking, and O. Buisson, *Phys. Rev. Lett.* **93**, 187003 (2004).
- [7] S. K. Dutta, *et al.*, *Phys. Rev. B* **78**, 104510 (2008).
- [8] E. Lucero, *et al.*, *Phys. Rev. Lett.* **100**, 247001 (2008).
- [9] J. M. Martinis, S. Nam, J. Aumentado, and C. Urbina, *Phys. Rev. Lett.* **89**, 117901 (2002).
- [10] K. J. Boller, A. Imamoglu, and S. E. Harris, *Phys. Rev. Lett.* **66**, 2593 (1991).

- [11] S. H. Autler and C. H. Townes, Phys. Rev. **100** 703 (1955).
- [12] K. Bergmann, H. Theuer, and B. W. Shore, Rev. Mod. Phys. **70**, 1003 (1998).
- [13] X. Xu, *et al.*, Science **317**, 929 (2007).
- [14] X. Xu, *et al.*, Nature Phys. **4**, 692 (2008).
- [15] G. Alzetta, A. Gozzini, L. Moi, and G. Orriols, Nuovo Cimento B **36**, 5 (1976).
- [16] K. V. Murali, Z. Dutton, W. D. Oliver, D. S. Crankshaw, and T. P. Orlando, Phys. Rev. Lett. **93**, 087003 (2004).
- [17] J. Siewert, and T. Brandes, Adv. in Solid State Phys. **44**, 181 (2004); arXiv:cond-mat/0506412.
- [18] While preparing the present manuscript, we became aware of a related, independent experiment which used a different superconducting system: M. Baur, *et al.*, arXiv:0812.4384.
- [19] R. W. Simmonds, *et al.*, Phys. Rev. Lett. **93**, 077003 (2004).
- [20] J. E. Field, K. H. Hahn, and S. E. Harris, Phys. Rev. Lett. **67**, 3062 (1991).
- [21] J. L. Picque and J. Pinard, J. Phys. B **9**, 77 (1976); J. E. Bjorkholm and P. F. Liao, Opt. Commun. **21**, 132 (1977).
- [22] C. Delsart and J.-C. Keller, J. Phys. B **9**, 2769 (1976).
- [23] B. P. Lanyon, *et al.*, Nature Phys. **5**, 134 (2009).